Journal of Scientific Research & Reports
3(12): 1642-1655, 2014; Article no. JSRR.2014.12.006

SCIENCEDOMAIN *international*
www.sciencedomain.org

Optical Properties of E-beam Evaporated Indium Selenide (InSe) Thin Films

J. Hossain[1*], M. Julkarnain[1], K. S. Sharif[1] and K. A. Khan[1]

[1]Department of Applied Physics and Electronic Engineering, University of Rajshahi, Rajshahi-6205, Bangladesh.

Authors' contributions

This work was carried out in collaboration among all authors. Author JH designed and carried out the experiments, results analysis and drafted the manuscript. Authors MJ and KSS conducted results analysis and managed the literature searches. Author KAK supervised the research and revised the results analysis and manuscript. All authors read and approved the final manuscript.

Original Research Article

Received 1st November 2013
Accepted 18th February 2014
Published 8th May 2014

ABSTRACT

Indium selenide (InSe) thin films were prepared by electron beam evaporation technique onto glass substrate at a pressure of ~8×10^{-5} Pa. The deposition rate of the InSe thin films is ~8.30 nms^{-1}. The XRD and SEM study reveal that InSe thin films are amorphous before phase-transition while they become polycrystalline after phase-transition. The Energy Dispersive Analysis of X-ray (EDAX) analysis shows that InSe thin films are non-stoichiometric. The change in electrical conductivity of InSe thin films with temperature shows a semiconducting behavior. The optical properties of both the virgin and phase-transited InSe thin films have been studied in the wavelength range $360<\lambda<1100$nm, respectively at room temperature. The study of absorption coefficient of virgin InSe thin films shows a direct type transition with a band gap of ≈1.65 eV which agrees well with the reported values. The variations of refractive index and dielectric constant of the films were also calculated and discussed in relation with film re-crystallization after heat treatment. The integrated values of luminous and solar transmittance as well as of reflectance suggest that InSe is a potential candidate for the application in selective surface devices.

**Corresponding author: E-mail: jak_apee@ru.ac.bd;*

Keywords: InSe thin film; e-beam technique; absorption coefficient; band tail; refractive index; dielectric constant.

1. INTRODUCTION

Indium selenide (InSe) is a layered semiconductor which has attracted much attention to be a new class of materials for solar energy conversion applications. The transport properties of InSe thin films have been widely investigated in the past years [1,2]. The near band-edge optical and electrical properties of strongly anisotropic crystals are subject of considerable technical interest. InSe thin film is of particular interest because the material has a variety of applications in optoelectronic devices [3], solar cells [4], and solid state batteries [5]. Literature reports indicate that InSe thin films have been prepared by a number of techniques by a number of researchers. These include vacuum evaporation [6-8], flash evaporation [9], molecular beam deposition [10], electro deposition [11], sol-gel method [12], etc. Despite of several studies on the growth and characterization of InSe thin films deposited by different methods there is a lack of understanding concerning the structure, optical and electrical properties which highly influence the device performance.

It is very important to study the optical properties of InSe thin films when these are to be used in devices particularly solar cells. In this paper, we discuss about the optical properties of InSe thin films prepared by electron beam evaporation technique onto glass substrate and compare the results with other researchers' works.

2. EXPERIMENTAL

Indium selenide (InSe) thin films were prepared by e-beam evaporation technique onto glass substrate at a pressure of ~8×10^{-5} Pa from InSe granular powder (99.999%) obtained from Materials by Metron, USA. All the films were deposited at room temperature. A detail of the sample preparations is reported elsewhere [13]. The film thickness was measured by the Tolanasky interference method with an accuracy of ±5nm [14].

3. RESULTS AND DISCUSSION

3.1 X-ray Diffraction (XRD) Study

The X-ray diffraction of the InSe thin films was done using a diffractometer, PHILIPS model "X'Pert PRO XRD System" [15]. The X-ray diffractograms of all the samples was recorded using monochromatic CuK_α radiation (λ=1.54187 Å), scanning speed 2 degree/min**,** starting from 8° and ending at 50° to confirm the information of the sintered product's single phase nature. The peak intensities were recorded with respect to their 2θ values.

The XRD patterns of the InSe thin films of thickness 300 nm are shown in Fig. 1 (a) and (b), respectively. It is observed from these patterns that the virgin films are amorphous in nature, while a number of remarkable peaks present in the phase-transited InSe films. So it is concluded that InSe thin films are amorphous before phase transformation while they become polycrystalline after structural transformation. These phenomena were also observed by other researchers [7,16,17].

The d_{hkl} values were calculated from the intensity peaks of the XRD spectra for InSe thin films [13]. These calculated values are compared with ASTM card's d_{hkl} values, and their

corresponding planes are (101), (420), (221), (100), (510) (1010). The XRD study reveals that the InSe thin films have polycrystalline hexagonal structure with the lattice parameters: a=19.20 Å, b=19.20 Å and c=4.00 Å, respectively.

From XRD data, the crystallite size and dislocation densities are calculated [13]. It is observed that the crystallite size varies from 18.034 to 109.025 nm, dislocation densities varies from 0.84×10^{14} to 30.746×10^{14}lin/m^2 and strain varies from 0.337×10^{-3} to 2.306×10^{-3} lin^{-2}.m^{-4} in the InSe thin films.

3.2 Scanning Electron Microscopy (SEM) and EDAX Study

Figs. 2(a) and (b) show the SEM images of the virgin and phase-transited InSe thin films of thickness 300 nm, respectively. These SEM images indicate that there is no sign of grains in the virgin films and the surfaces are almost smooth and uniform. While in the phase-transited InSe thin films the surfaces are rough.

The analysis of the elemental compositions for the InSe thin films of various thicknesses were estimated by using the method of Energy Dispersive Analysis of X-ray (EDAX). The EDAX spectra of the virgin and phase-transited InSe thin films of thickness 240nm is shown in Figs. 3 (a) and (b), respectively.

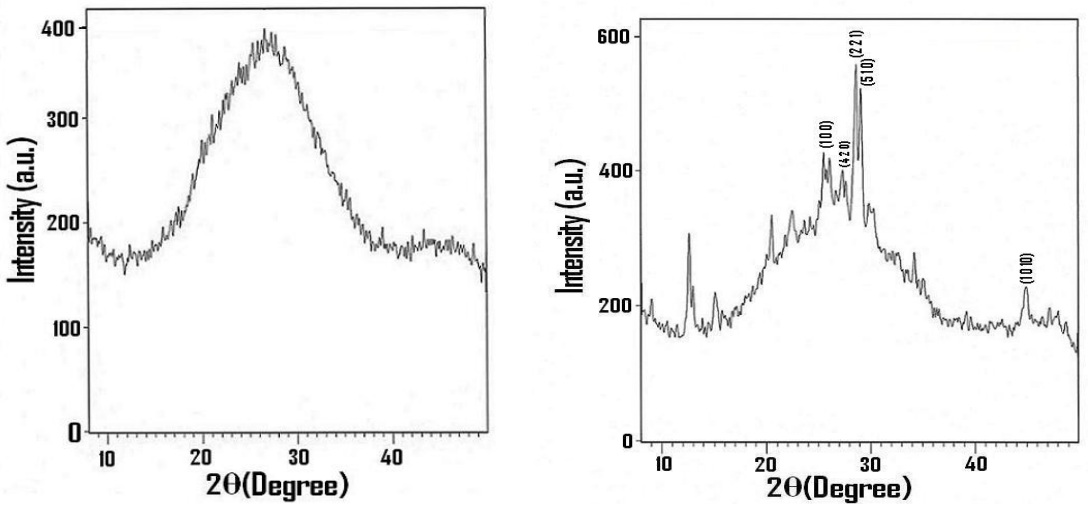

Fig. 1. XRD spectra for (a) virgin and (b) phase-transited InSe thin films of thickness 300nm

Table 1 shows the elemental composition of InSe thin films of thicknesses of 240 and 300nm respectively. The result of EDAX study shows that InSe thin films are non-stoichiometric [13].

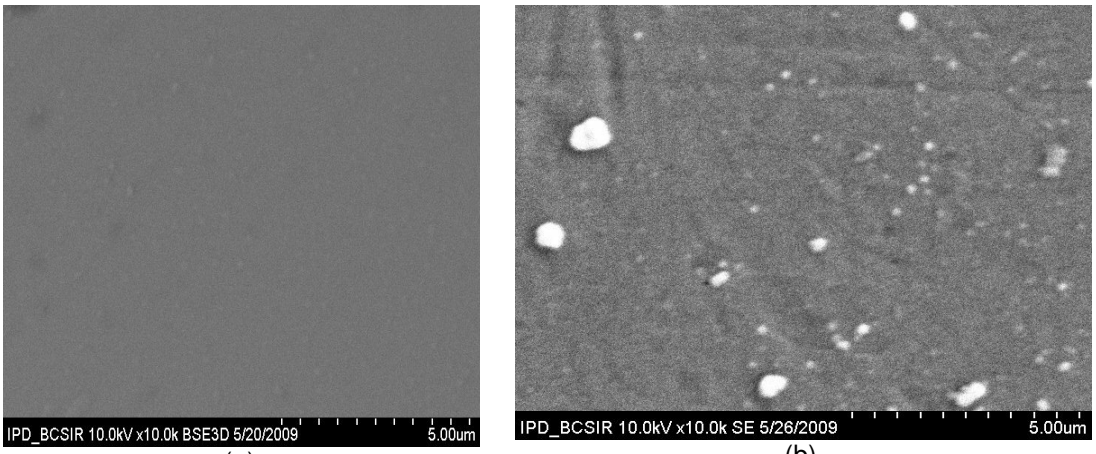

(a) (b)

Fig. 2. The SEM images of (a) virgin and (b) phase-transited InSe thin films of thickness 300nm

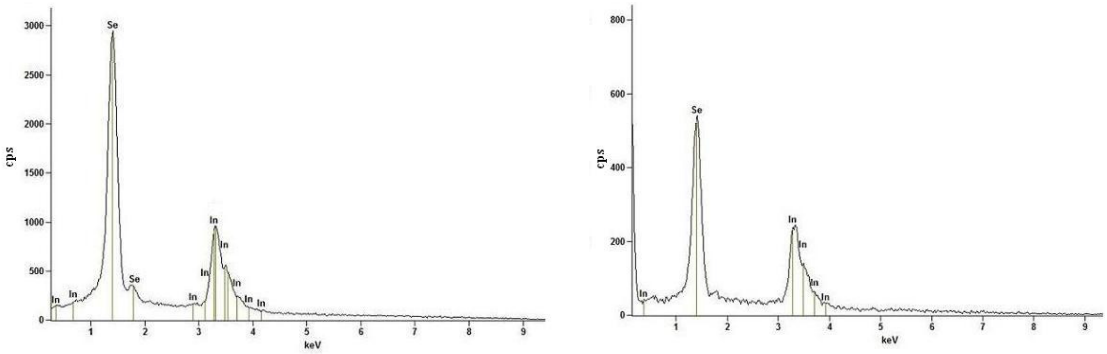

(a) (b)

Fig. 3. The EDAX spectra for (a) Virgin and (b) Phase-transited InSe thin films of thickness 240 nm

Table 1. The elemental composition of InSe thin films of different thicknesses

Thickness (nm)	EDAX Results		Remarks
	In(%wt)	Se(%wt)	
240	70.68	29.32	Virgin
	70.75	29.25	Phase-transited
300	70.05	29.95	Virgin
	70.58	29.42	Phase-transited

3.3 Electrical Properties of InSe Thin Films

The change in the electrical conductivity was investigated for the virgin InSe thin films [13]. The electrical conductivity was measured as a function of temperature T in the 305-475K range. The conductivity was measured by applying a d. c. 0-15 V bias across the films with silver contact and recording the current and voltage simultaneously by using a standard four-probe van-der-Pauw technique. It was seen from the study that the conductivity increases

continuously with temperature and there is a sharp increase in conductivity at a temperature within the range which slightly varies with film thickness. This phase change in conductivity was observed to be irreversible, i.e., it did not return to the initial state. The irreversible temperature dependence of electrical conductivity reveals the changes in the film structure during heat treatment and improvement in the crystallinity of the film [7,16,17].

3.4 Optical Properties of InSe Thin Films

The transmittance and reflectance of virgin and phase-transited InSe thin films of thicknesses 175, 240 and 300nm are shown in Fig. 4 and 5, respectively [15].

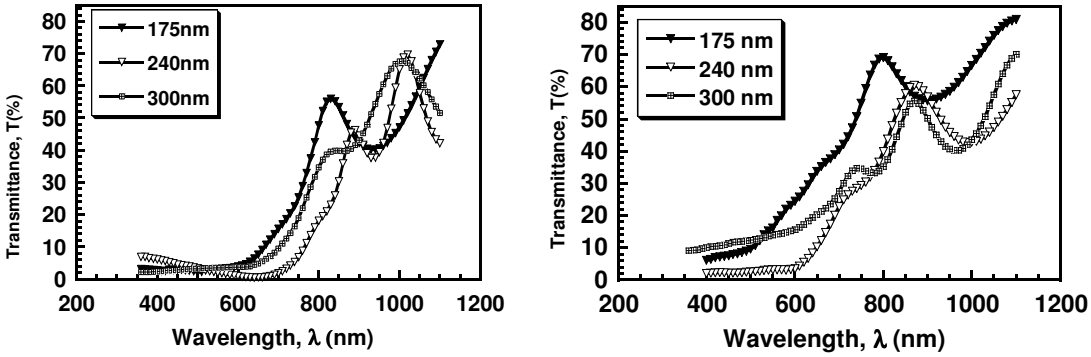

Fig. 4. Variation of transmittance with wavelength of (a) virgin and (b) phase-transited InSe films of different thicknesses

It is observed from the above figures that the transmittance tends to zero in the ultra-violet region and increases with wavelength in the visible range. This may happen due to the fact that when the photon energy is equal or greater than the band gap energy of the InSe thin films photons are highly absorbed by the films. From the figure it is also seen that the absorption edge shifts towards the higher wavelength side with increase in the film thickness with exception for 300nm, which may happen due to surface imperfections. This indicates that the band gap value decreases with increase of film thickness. Like transmittance, reflectance is relatively low in the ultra-violet region and in the visible and IR regions values vary due to interference.

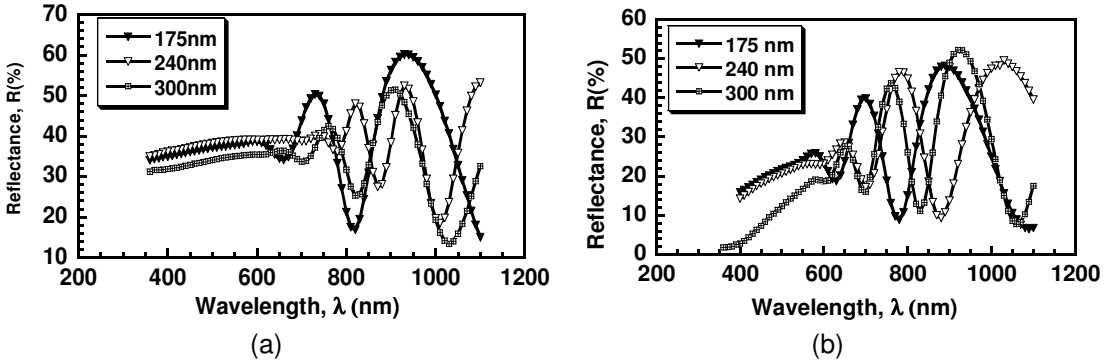

Fig. 5. Variation of reflectance with wavelength of (a) virgin and (b) phase-transited InSe films of different thicknesses

Figs. 6 (a) and (b) show the variation of absorption coefficient with photon energy for both the virgin and phase-transited InSe thin films respectively. It is found that the absorption coefficient increases at higher energy (>1.5 eV). This increased absorption near the absorption edge is caused by the transition of electron from the valance band to conduction band.

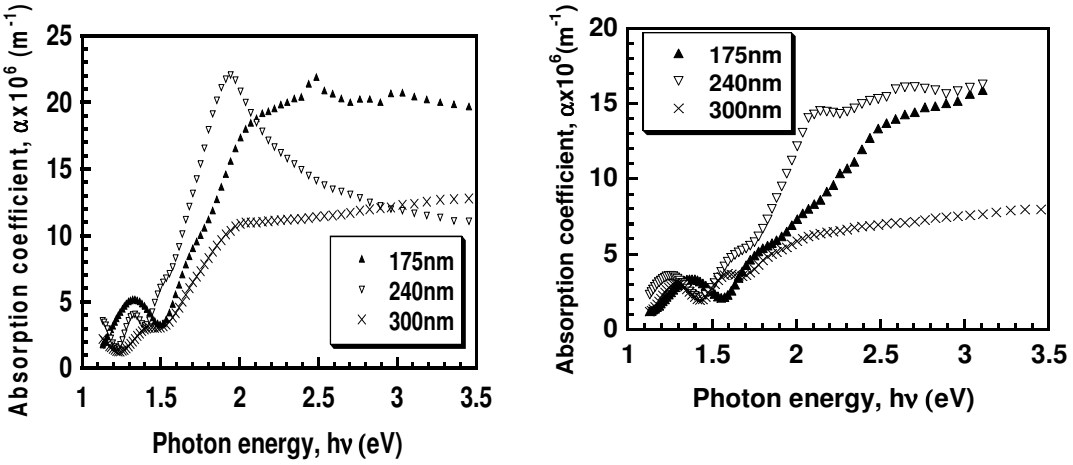

Fig. 6. Variation of absorption coefficient with photon energy of (a) virgin and (b) phase-transited InSe thin films of different thickness

3.4.1 Optical band gap

In the high absorption region, absorption coefficient (α) can be represented by the relation as Tauc [18] and Pankove [19], respectively,

$$\alpha h\upsilon = A(h\upsilon - E_g)^n \tag{1}$$

where, A is constant depending on the transition probability, E_g is the optical band gap and n is an index that characterizes the optical absorption process and is theoretically equal to 2, 1/2, 3 or 3/2 for indirect allowed [20], direct allowed, indirect forbidden and direct forbidden transitions, respectively. The usual method for determining the value of the band gap E_g is obtained from a graph of $(\alpha h\nu)^{1/n}$ versus photon energy, $h\nu$. If an appropriate value of n is used to obtain a linear plot, the value of E_g will be given by the intercept on the $h\nu$ axis. Fig. 7 shows the plot of $(\alpha h\nu)^2$ vs. hν for (a) virgin and (b) phase-transited InSe thin film of thickness of 300nm. Table 2 shows the variations of direct band gap with thickness the InSe thin films [15].

Table 2. The optical band gap of InSe thin films

Thickness, t (nm)	Virgin thin films	Phase-transited thin films
	Direct band gap (eV)	Direct band gap (eV)
175	1.65	1.92
240	1.64	1.76
300	1.60	1.68

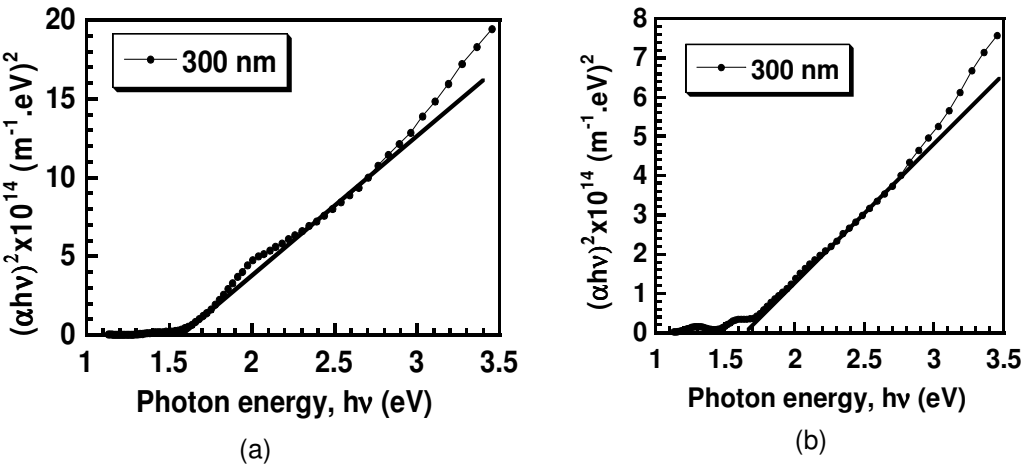

Fig. 7. The plot of $(\alpha h\nu)^2$ vs. hν for (a) virgin and (b) phase-transited InSe thin film of thickness of 300nm

The calculated values of direct band gap (E_g) for different thickness of virgin InSe samples vary between 1.60 to 1.65 eV which agrees well with early reports [7,21,22]. It is shown from the table that band gap slightly decreases with thickness. This decrease of band gap with thickness may be attributed to the presence of unstructured defects, which increase the density of localized states in the band gap and consequently decrease the energy gap [23]. The calculated values of direct band gap (E_g) for different thickness of phase-transited InSe samples vary between 1.68 to 1.92 eV.

Fig. 8 shows the variation of direct band gap of both the virgin and phase-transited (after heating the samples) InSe thin films with thickness. The observed change of band gap of the virgin and phase-transited films can be partially explained- on the basis of the model of the density of states in amorphous solids proposed by Mott and Davis [24]. According to this model, the width of the localized states near the mobility edges depends on the level of disorder and defects present in the amorphous structure. In particular, it is known that unsaturated bonds together with some saturated bonds are produced as a result of non-stoichiometry of the components in the amorphous films. In the process of heated films (i.e. in polycrystalline films), the unsaturated defects are gradually annealed out producing a large number of saturated bonds. The reduction in the number of unsaturated defects decreases the density of localized states in the band structure, consequently increasing the optical band gap [13,25].

3.4.2 Refractive index and dielectric constant

The refractive index and dielectric constant can be calculated from the transmittance (T) data using Murman theory [26]. Figs. 9 (a) and (b) reveal the dependence of refractive index on wavelength of virgin and phase-transited InSe thin films. It is seen from the figures that for the virgin films refractive index ranges from 1.3 to 2.13 and for the phase-transited films it ranges from 1.22 to 1.71. At lower wavelength (400nm) region, the refractive index increases and at higher wavelength (800nm) region it decreases. The increase of refractive index in the lower wavelength region may be due to the strong effect of surface and volume imperfections on the microscopic scale [7].

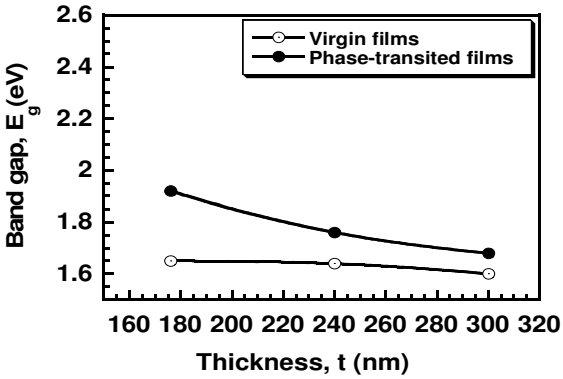

Fig. 8. Variation of optical band gap with thickness for InSe thin films

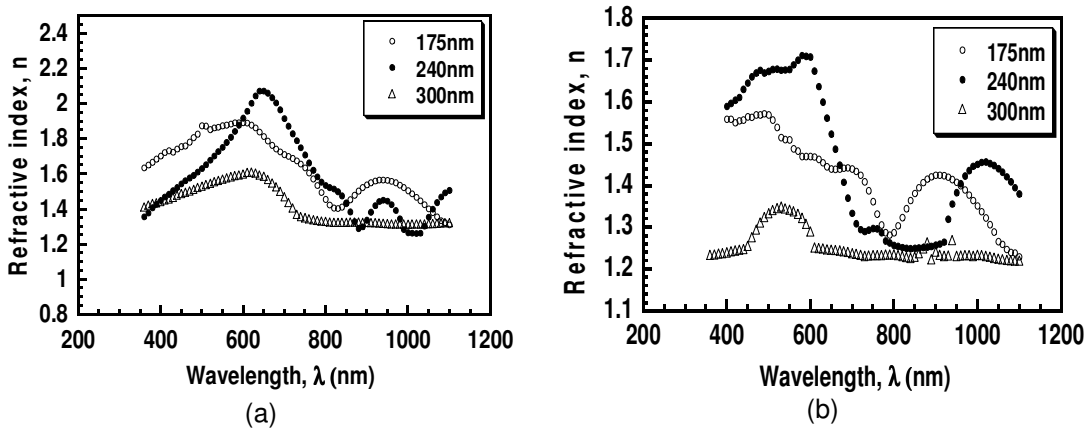

Fig. 9. Dependence of refractive index on the wavelength for (a) virgin and (b) phase-transited InSe thin films

The dependence of dielectric constant on wavelength for both the virgin and phase-transited InSe thin films of different thicknesses is shown in Fig. 10 (a) and (b), respectively. It is seen from the graphs that for the virgin films dielectric constant ranges from 1.58 to 4.30 and for the phase-transited films it ranges from 1.5 to 2.9.

3.4.3 Urbach tail calculation for InSe thin films

According to Tauc [18], it is possible to separate three distinct regions in the absorption edge spectrum of amorphous semiconductors. The first weak absorption tail, which originates from defects and impurities; the second is the exponential edge region, which is strongly related to the structural randomness of the system and the third is the high absorption region that determines the optical energy gap. Below 2.0 eV, the absorption coefficient α indicates a long band tail in the absorption curves, which may cause due to defects and impurities of the samples [27].

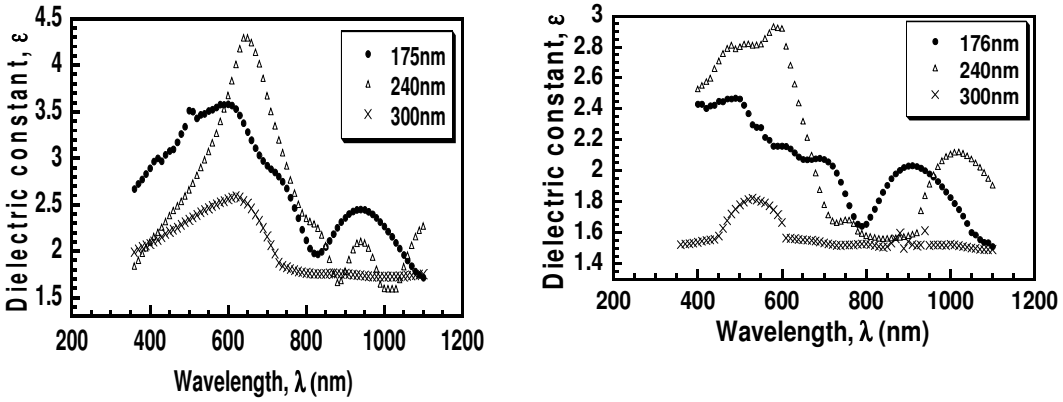

Fig. 10. Dependence of dielectric constant on the wavelength for (a) virgin and (b) phase-transited InSe thin films

In the exponent edge where the absorption coefficient α lies in the absorption region of $3.08\times10^{6}<\alpha<20.85\times10^{6}$ m^{-1} (From Figs. 6(a) and 6(b)), the absorption coefficient is governed by the relation as Urbach law [28].

$$\alpha = \alpha_0 \exp(h\nu / E_e) \tag{2}$$

where α_0 is a constant, hν is incident photon energy and E_e is the width of the band or Urbach tail. Using equation 2, the obtained data of $\ln\alpha$ has been plotted as a function of photon energy $h\nu$, which is shown in Fig. 11. The calculated Urbach tail of InSe thin films of different thicknesses is shown in Table 3.

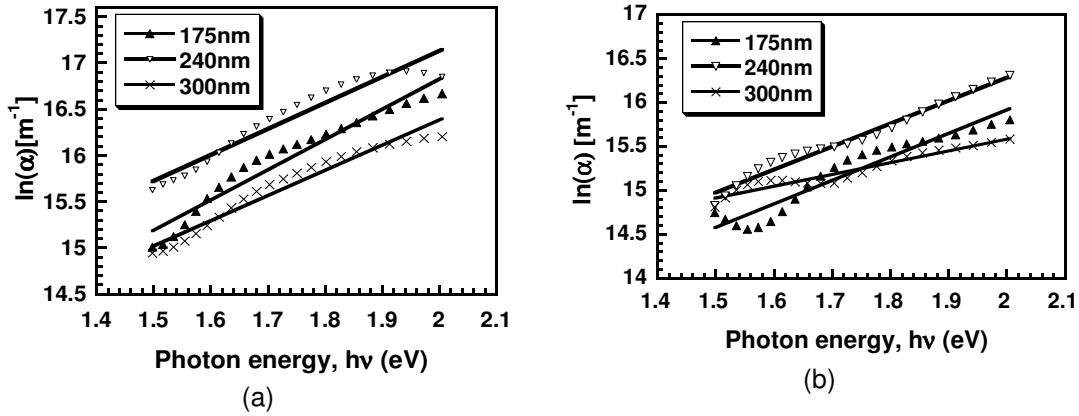

Fig. 11. The plots of ln(α) vs. photon energy for (a) virgin and (b) phase-transited InSe thin films of different thicknesses

Table 3. Urbach Tail of InSe Thin Films

Film thickness (nm)	Urbaich tail, E_e(eV)	
	Virgin films	Phase-transited films
175	0.52	0.73
240	0.33	0.77
300	0.47	1.40

3.4.4 Photoluminescence (PL) study of InSe thin films

The photoluminescence (PL) spectra of different InSe thin films have been measured at an excitation wavelength of 400nm whose corresponding energy is well above the band gap of the samples.

Figs. 12 (a) and (b) indicate the PL spectra of virgin and phase-transited InSe thin films of various thicknesses. It is observed from the figures that the PL spectra are very sharp with a narrow band of about 25nm. It is evident from the figures that the peak shifts depending on the film thickness. This peak shifting may occur due to the decrease of band gap with thickness of the InSe thin films.

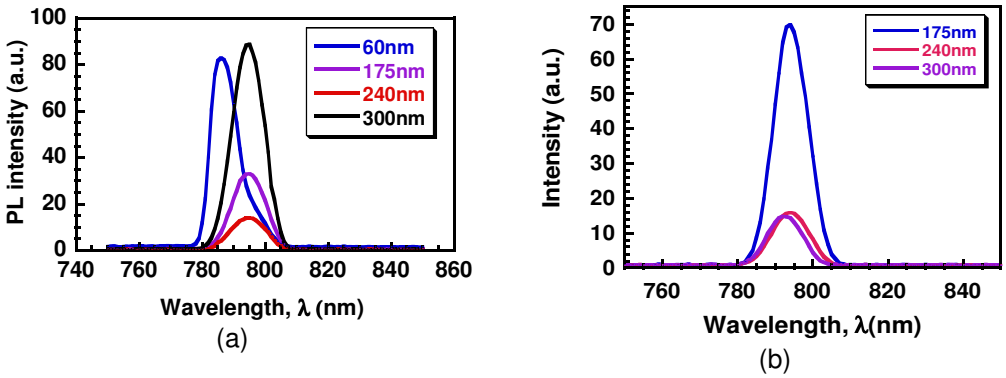

Fig. 12. Thickness dependency of PL peak position and peak height of (a) virgin and (b) phase-transited InSe thin films of different thickness

3.4.4.1 Band gap determination from the PL spectra

The energy band gap of InSe thin films has been calculated from the PL spectra at room temperature. In the case of indirect transitions, the radiation intensity can be described by equation [29].

$$I(h\nu) \approx \nu^2 (h\nu - E_g^i)^2 \exp[-\frac{(h\nu - E_g^i)}{K_B T}] \quad (3)$$

where, I is the radiation intensity, v is the light frequency, h is the Plank constant, E_g^i is the indirect band gap of InSe, K_B is the Boltzmann constant, T is the absolute temperature.

For direct transitions, the spectrum of intrinsic radiation has a form [29].

$$I(h\nu) \approx \nu^2 (h\nu - E_g^d)^{1/2} \exp[-\frac{(h\nu - E_g^d)}{K_B T}] \quad (4)$$

where E_g^d is the direct band gap of InSe.

Attempts have been taken to calculate both the indirect and direct band gap using equation 3 and 4, but the best fit has been observed for direct band gap.

The band calculated according to equation 4 has been shown in Fig. 13 for virgin thin films of thicknesses 240 and 300nm, respectively. As there is no peak shift between virgin and phase-transited film of same thickness, band calculation is not shown for phase-transited films. The direct band gaps of virgin InSe thin films calculated from PL spectra are shown Table 4.

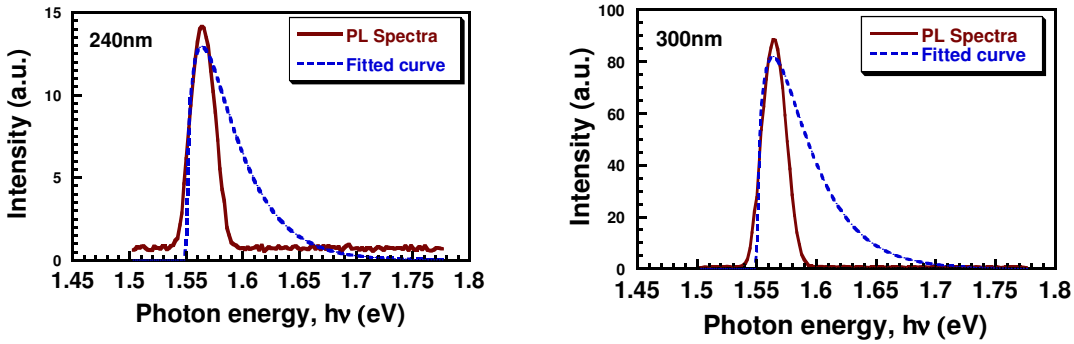

Fig. 13. Comparison of PL spectra with calculated spectra of virgin InSe thin films of 240 and 300nm, respectively

Table 4. The band gap of virgin InSe thin films from PL Spectra

Film thickness (nm)	Direct band gap (eV)
60	1.60
175	1.57
240	1.56
300	1.55

It is seen from the table that the band gap values range between 1.55 and 1.60, respectively which closely agrees with the band gap obtained from the optical study. A similar observation on PL spectra of InSe thin films has been done by V.M. Katerynchuk et al. [30] with a slightly different band gap.

3.4.5 Selective surface study

For measuring the performance of coating in selective surface applications, it is convenient to introduce certain integrated optical quantities. These are especially the luminous (lum) and solar (sol) properties obtained from

$$X_\rho = \frac{\int d\lambda \Phi_\rho X(\lambda)}{\int d\lambda \Phi_\rho(\lambda)} \tag{5}$$

Where X denotes transmittance or reflectance. The luminous quantities are obtained by setting $\Phi_\rho = \Phi_{lum}$ equal to the standard luminous efficiency function for photooptic vision [31] as specified CIE (Commission International de l'Éclairage). For solar quantities, one can use $\Phi_\rho = \Phi_{sol}$, according to the tabulated AM2 irradiance spectrum [32]. This calculation has been done for different film thicknesses. The integrated values of luminous and solar transmittance as well as reflectance were calculated [15]. The calculated $\%T_{sol}$, $\%R_{sol}$ and $\%T_{lum}$, $\%R_{lum}$ are tabulated in Table 5.

Table 5. $\%T_{sol}$, $\%R_{sol}$, $\%T_{lum}$, and $\%R_{lum}$ values for virgin and phase-transited InSe thin films

Film thickness (nm)	Solar		Luminous		Remarks
	$\%T_{sol}$	$\%R_{sol}$	$\%T_{lum}$	$\%R_{lum}$	
175	20.35	38.49	3.32	37.74	
240	14.42	37.90	1.97	38.80	Virgin films
300	19.20	33.77	3.60	35.02	
175	38.14	25.78	18.16	23.25	
240	21.97	27.42	3.31	22.78	Phase-transited
300	26.49	40.04	14.34	16.97	films

It is seen from the table that the integrated luminous and solar transmittance and of reflectance vary anomalously with increasing film thicknesses. Appreciable order of transmittance and reflectance indicate its potential candidacy for the application in selective surface devices.

4. CONCLUSION

InSe thin films were prepared by electron beam evaporation technique onto glass substrate. The deposition rate of the films was ~8.30 nms^{-1}. The XRD study shows that the virgin films are amorphous in nature while they transform to polycrystalline nature after heat-treatment. The SEM study of InSe thin films shows that before phase-transition there are no grains in the films and the surfaces are almost smooth while the surfaces are rough after phase-transition. The EDAX study shows a non-stoichiometric InSe thin film. The electrical conductivity of the films shows a semiconducting behavior. The optical study shows a direct band gap of ≈1.65 eV of the films which is well agreed with the other reported values. It is also noticed that the band gap increases in the phase-transited films as compared to the virgin films. Notable order of luminous and solar transmittance and reflectance indicate the potential candidature of the InSe thin films for application in the selective surface devices.

ACKNOWLEDGEMENTS

One of us, J. Hossain is indebted to Mrs. Nazia Sultana, SEM Operator, BCSIR, Dhaka, Bangladesh for her kind help during the study of SEM and EDAX and Professor Abu Bakar

Md. Ismail, Dept. of Applied Physics & Electronic Engineering, University of Rajshahi, Bangladesh for his valuable suggestions.

COMPETING INTERESTS

Authors have declared that no competing interests exist.

REFERENCES

1. Errandonea D, Segura A, Sanchez-Royo JF, Munoz V. Investigation of conduction-band structure, electron-scattering mechanisms, and phase transitions in indium selenide by means of transport measurements under pressure. Physical review B. 1997;55(24):16217-16225.
2. Segure A, Mari B, Martinez-Pastor J, Chevy A. Three-dimensional electrons and two-dimensional electric subbands in the transport properties of tin-doped *n*-type indium selenide: Polar and homopolar phonon scattering. Phys. Rev. B. 1991;43(6):4953-4965.
3. De Blassi C, Micocci G, Rizzo A, Tepore A. Large InSe single crystals grown from stoichiometric and non-stoichiometric melts. J. Crystal Growth. 1982;57:482-486.
4. Lang O, Rudolph R, Klein A, Pettenkofer C, Jaegerman W, Sánchez J, Segura A, Chevy A. Proceedings of the E. C. Photovoltaic Solar Energy Conference (Reidel, Dordrecht) page- 2023; 1996.
5. Gomes da Costa P, Balkanaski M, Wallis RF. Effect of intercalated lithium on the electronic band structure of indium selenide. Phys. Rev. B. 1991;43:7066-7069.
6. Peršin M, Čelustka B, Markovič B, Peršin A. Some electrical and optical properties of InSe thin films. Thin Solid Films. 1970;5:123-128.
7. Viswanathan C, Rusu GG, Gopal S, Mangalaraj D, Sa. K. Narayandass. On the electrical characteristics of vacuum evaporated indium selenide thin films. J of Optoelectronics and Advanced Materials. 2005;7:705-711.
8. Di Giulio M, Micocci G, Rella R, Siciliano P, Tepore A. Optical absorption and photoconductivity in amorphous indium selenide thin films. Thin Solid Films. 1987;148:273-278.
9. Peršin M, Peršin A, Čelustka B. Effect of thermal treatment on the properties of flash evaporated thin films of InSe. Thin Solid Films. 1972;12:117-122.
10. Emery JY, Brahim-Otsmane L, Jouanne M, Julien C, Balkanski M. Growth conditions of In_xSe_y films by molecular beam deposition. Materials Science and Engineering B. 1989;3:13-17.
11. Gopal S, Viswanathan C, Karunagara B, Sa. K. Narayandass, Mangalaraj D, Junsin Yi. Preparation and characterization of electrodeposited indium selenide thin films. J of Cryst. Res. Technol. 2005;40:557-562.
12. Mutlu IH, Zarbaliyev MZ, Aslan F. Indium selenide thin film prepared by sol-gel technique. J of Sol-Gel Science and Technology. 2007;43:223-226.
13. Hossain J, Julkarnain M, Sharif KS, Khan KA. Crystallization of e-beam evaporated amorphous InSe thin films after heat-treatment. International Journal of Renewable Energy Technology Research. 2013;2(9):220–226.
14. Tolansky S. Multiple beam interferometry of surface and films, London: Oxford University Press; 1948.
15. Hossain J, Julkarnain M, Sharif KS, Khan KA. Preparation and Properties of Indium Selenide (InSe) Thin Films for Selective Surface Applications. Journal of Physical Science and Application. 2011;1:37-43.

16. Grigorov SN, Kosevich VM, Kosmachev SM, Taran AV. Crystallization of the Amorphous Indium Selenide Films during Annealing. Physics and Chemistry of Solid State. 2004;5:35-37.
17. Rusu GG. On the electrical and optical properties of nano crystalline CdTe thin films. J of Optoelectronics and Advanced Materials. 2001;3(4):861-866.
18. Tauc J. Amorphous and liquid semiconductors, New York: Plenum Press, Chap. 1974;4.
19. Pankove JI. Optical processes in semiconductors, New Jersey: Prentice-Hall, 1971;93.
20. Savitskii AV, Kurik MV, Tovstyuk KD. Optical absorption in Zn, HgI, Te thin films. Opt. Spectrose. 1964;19:56-73.
21. Viswanathan C, Senthilkumar V, Sriranjini R, Mangalaraj D, Sa. K. Narayandass, Junsin Yi. Effect of substrate temperature on the properties of vacuum evaporated indium selenide thin films. Crystal Research and Tech. 2004;40:658-664.
22. Qasrawi AF. Temperature dependence of the band gap, refractive index and single-oscillator parameters of amorphous indium selenide thin films. Optical Materials. 2007;29:1751-1755.
23. El-Zahed H, El-Korashy A, Abdel Rahman M. Effect of heat treatment on some of the optical parameters of $Cu_9Ge_{11}Te_{80}$ films. Vacuum. 2003;68:19-27.
24. Mott NF, Davis EA. Electronic Process in non-crystalline materials, 2nd Edn, Clarendon Press, Oxford; 1979.
25. Parlak M, Erçelebi Ç. The effect of substrate and post-annealing temperature on the structural and optical properties of polycrystalline InSe thin films. Thin Solid Films. 1998;322:334-339.
26. Murmann H. Die optischen Konstanten durchsichtigen Silbers. Zeitschrift für Physik A Hadrons and Nuclei. 1933;80(3-4):161-177.
27. Qasrawi AF. Refractive index, band gap and oscillator parameters of amorphous GaSe thin films. Cryst. Res. and Technol. 2005;40(6):610-614.
28. Urbach F. The Long-Wavelength Edge of Photographic Sensitivity and of the Electronic Absorption of Solids. Phys. Rev. 1953;92(5):1324-1324.
29. Sze CM. In Physics of semiconductor devices, John Wiley and Sons, New York; 1969.
30. Katerynchuk VM, Kovalyuk MZ, Tovarnitskii MV. Photoemission spectra of indium selenide. Semiconductor Physics, Quantum Electronics and Optoelectronics. 2006;9(4):36-39.
31. Wyszecki G, Stiles WS. Color Science, 2nd Edt. Wiley & Sons, New York; 1982.
32. Moon P. Proposed standard solar-radiation curves for engineering use. J of the Franklin Inst. 1940;230:583-617.

Peer-review history:
The peer review history for this paper can be accessed here:
http://www.sciencedomain.org/review-history.php?iid=517&id=22&aid=4518